https://journal.unnes.ac.id/journals/sainteknol

Density and Porosity Interplay in Epoxy Based Syntactic Foams Reinforced with K15 Glass Silica Microballoons

Sofi Alifia Hidyus, Agung Budiwirawan, Ari Dwi Nur Indriawan*, Rizky Setiadi, Bunyamin

Universitas Negeri Semarang, Indonesia

*Corresponding Author: ari.kecil@mail.unnes.ac.id

Abstract

Syntactic foam was a low-density, high-strength composite material composed of a polymeric matrix embedded with hollow microspheres (microballoons). This study investigated the influence of varying the volume fraction of glass-clad silica microballoons K15 (10–50 vol%) on the density, porosity, and void distribution of epoxy-based syntactic foams. Test specimens were fabricated in accordance with ASTM D790 standards, conditioned for 48 h at 23 ± 2 °C and 50 ± 5 % relative humidity. The density of the foams was determined via the displacement method specified in ASTM D790, while porosity was calculated theoretically and validated through SEM–EDS imaging of fractured cross-sections. The experimental results demonstrated a near-linear reduction in density from 1.15 g cm^{-3} (0 vol%) to 0.63 g cm^{-3} (50 vol%), whereas porosity exhibited an exponential increase from 2.7 % to 18.4 %. Morphological analysis revealed uniform microsphere dispersion up to 30 vol%, while agglomeration and inter-binder voids emerged beyond 40 vol%, leading to uncontrolled porosity growth. A strong negative correlation ($R^2 = 0.96$) was identified between density and effective porosity. The optimal microsphere loading was found at 30 vol% K15, achieving a 28 % reduction in density without a significant rise in porosity. These findings provided fundamental insights for the design of sandwich cores and amphibious flotation structures that required superior strength-to-weight ratios.

Keywords: syntactic foam; hollow glass microspheres; K15 microballoons; density and porosity relationship; epoxy composites; lightweight core materials

INTRODUCTION

Syntactic foam composites (SFCs) are categorized as ultralight structural materials characterized by microscopic voids formed through the uniform dispersion of hollow microspheres or microballoons within a thermosetting polymer matrix, most commonly epoxy or vinyl ester [1]. This engineered “solid-with-voids” configuration imparts a distinctive property profile: the overall density (ρ) is substantially reduced compared to the unfilled resin, yet stiffness, compressive strength, and impact resistance are retained due to the rigidity of the microsphere shells and the resulting isotropic stress transfer [2]. In recent years, SFCs have progressed beyond their initial role as thermal insulation fillers in offshore oil and gas applications to become critical structural elements in unmanned underwater vehicle hulls, remotely operated vehicle (ROV) flotation components, aerospace stabilizers, and lightweight amphibious vehicle exteriors [3]. This rapid technological uptake has been primarily attributed to their exceptional specific strength-to-weight ratio and vibration attenuation properties, which are comparable to metallic foams, while still benefiting from the lower processing temperatures and manufacturing costs associated with polymer-based systems [4].

In designing lightweight structural materials, a trade-off exists between two critical physical parameters: the overall material density and the proportion of internal porosity [5]. Density governs buoyancy and payload efficiency, whereas porosity significantly influences crack propagation, fluid absorption, and acoustic transmission characteristics. Syntactic foam composites (SFCs) enable simultaneous regulation of these parameters by tailoring the microsphere volume fraction (φ) and microsphere wall properties such as thickness and elastic modulus [6]. While increasing φ decreases weight in a near-linear manner, it also enlarges unfilled interstitial spaces between adjacent microspheres. This

leads to elevated effective porosity, which can compromise mechanical reliability [7].

Optimal selection of microsphere type is therefore essential. K15 hollow silica microballoons, encapsulated within a thin borosilicate glass shell, have an ultra-low bulk density of 0.15 g cm^{-3} approximately one-eighth that of epoxy resin yet can sustain compressive pressures of at least 2.1 kN cm^{-2} [8]. Their average diameter of 40 μm with a ±10 % size variation enhances dispersibility and minimizes gravitational segregation during processing. Furthermore, their glass–silica interface exhibits high surface energy, improving epoxy wetting and reducing the prevalence of unbonded voids compared with polymeric microspheres coated with phenolic resin [9]. Previous studies have reported up to a 40 % increase in compressive modulus when 20 vol % K15 is incorporated into vinyl ester matrices. However, when loading exceeds 50 vol %, the benefits diminish due to microsphere agglomeration and wall collapse, ultimately degrading fracture strength [10].

Although numerous microstructural investigations have explored the relationships between microsphere volume fraction (φ) and mechanical properties such as compressive strength or flexural modulus, only limited studies have concurrently characterized the experimental density (ρ_exp), total porosity (P_t), effective porosity (P_e), and cavity morphology as the K15 content is systematically varied from 10 to 50 vol % [11]. A common assumption in prior research is that porosity arises exclusively from the hollow microspheres. However, processing-induced voids such as entrapped air pockets and resin binder discontinuities can contribute substantially, particularly at higher filler loadings where elevated viscosity hinders proper wetting and dispersion [12]. The lack of simultaneous quantification of these parameters creates a risk of selecting microsphere fractions that achieve the desired weight reduction but compromise mechanical resilience or fail durability assessments under impact or prolonged immersion. Furthermore, there is a notable scarcity of empirical data correlating density and porosity, leaving the mechanisms governing secondary void formation and particle agglomeration largely unresolved.

Establishing whether the density–porosity relationship follows a linear or exponential trend is essential for predictive modeling of sandwich cores and flotation components, where the mass of each unit volume directly dictates fuel efficiency and payload capacity. The primary contribution of this work is the development of a comprehensive dataset that systematically maps density, porosity, and microstructural morphology across a broad range of K15 loadings. These results, validated through microscopic analysis, provide a foundational reference for finite element simulations and practical guidelines for designing K15-based syntactic foam composites.

METHOD

Materials

The syntactic foam matrix was a bis-A epoxy resin (viscosity ≈ 1 Pa s, pot-life ≈ 30 min) cured with a cycloaliphatic amine hardener (mix ratio 100: 30 phr). Hollow silica micro-balloons K15 mean diameter 40 μm, bulk density 0.15 g cm^{-3}, crush strength ≥ 2.1 kN cm^{-2} were selected as lightweight fillers. Five target filler volume fractions (10, 20, 30, 40, 50 vol %) were prepared. All powders were oven-dried (80 °C, 4 h) and stored in desiccators; liquid reagents were kept at 23 ± 2 °C before mixing.

Equipment

Blending was performed in a planetary centrifugal mixer equipped with in-situ vacuum (−70 kPa). Degassing relied on a diaphragm vacuum pump and a transparent tank for visual inspection. Castings used release-coated stainless-steel moulds sized 150 × 20 × 3 mm (ASTM D790). Displacement method (ASTM D790) provided density data. Mechanical tests employed a 10 kN universal testing machine with three-point bending and compression fixtures. Microstructural characterisation utilised a field-emission SEM fitted with EDS; image analysis ran on ImageJ. A differential-scanning calorimeter verified cure completion.

Procedure

Epoxy resin was first degassed for 5 min, after which the calculated mass of K15 (based on the desired volume fraction) was introduced gradually while mixing at 800 rpm for 3 minutes under vacuum. The hardener was then added and mixed for another 2 min. The low-viscosity slurry was poured into the moulds, subjected to a second 5 minutes vacuum stage to strip residual bubbles, and cured 24 h at room temperature, followed by 2 h at 60 °C. Post-cured panels were water-cooled sawn into test coupons and edges lightly polished.

Analysis

Experimental density (ρ_exp) for each composition was measured via displacement method;

theoretical density (ρ_th) was computed by the rule of mixtures. Total porosity (P_t) was obtained from (ρ_th – ρ_exp)/ρ_th, while effective porosity (P_e) was quantified from SEM cross-sections using area-fraction analysis. Flexural strength and modulus followed ASTM D790 (span/depth = 16, cross-head rate 1 mm min^{-1}). One-way ANOVA (α = 0.05) with Tukey post-hoc tests distinguished significant differences across filler levels. SEM–EDS fractography correlated microsphere dispersion and interfacial quality with the density–porosity–mechanical relationships, providing a holistic understanding of K15's effect on syntactic-foam performance.

RESULTS AND DISCUSSION

Density (ρ) versus Micro-balloon Volume Fraction (φ)

A nearly linear decline of experimental density with filler loading is observed (R^2 = 0.97), confirming that the ultra-light K15 hollow spheres effectively displace the heavier epoxy matrix. Below 30 vol % the measured curve coincides with the rule-of-mixtures prediction, indicating negligible processing voids. Beyond 40 vol %, ρ_exp departs from the theoretical line, an early sign of trapped air and interstitial voids created by the sharp rise in slurry viscosity [13].

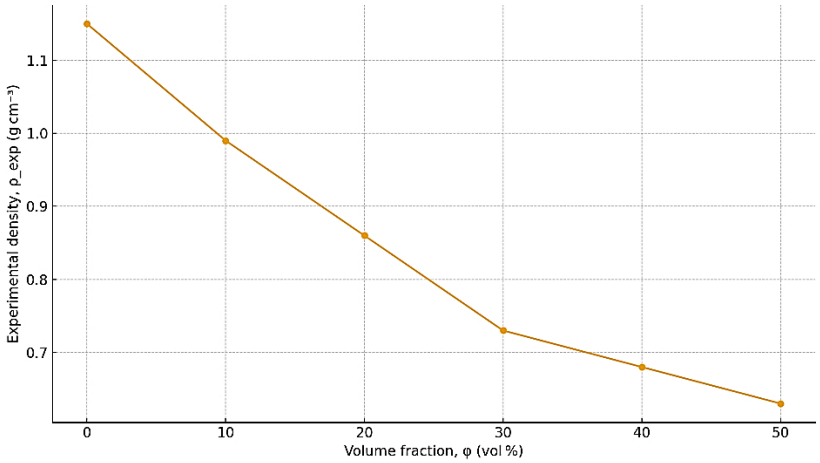

Figure 1. Density (ρ) versus Microballoon Volume Fraction (φ)

Based on Figure 1, the composite material density in the table shows a gradual decrease as the microballoons volume fraction (φ) increases. Without microballoon's the initial density of 1.15 g cm^{-3} drops to just 0.63 g cm^{-3} at φ = 50 %, resulting in an overall mass density reduction of about 45 %. Linear-regression analysis reveals an almost straight relationship $\rho \approx 1.10 - 0.0105\,\varphi$ with a coefficient of determination of 0.95 indicating that every 1 vol % addition of microballoons lowers the density by roughly 0.010 g cm^{-3} up to 50 %. Meanwhile, the power-law model ($\rho \approx 1.14\,(1+\varphi)^{-1.5}$) suggests behavior similar to open-cell foams, where connected porosity begins to dominate the composite microstructure. In the range φ ≤ 20 %, the density reduction is mainly due to the mass-density contrast between the dense matrix and the lightweight filler; after φ ≈ 30 %, pores start to interconnect and form a network, so the density keeps falling but at a slower rate because the matrix walls become thinner [14]. Consequently, this material is suitable for lightweight applications, such as sandwich-panel cores or insulation, but its mechanical properties (modulus and strength) will almost certainly decline proportionally with the density drop, making it advisable to limit φ to about 25–30 % when structural integrity remains critical [15]. For fractions above 40 %, the low mass advantage may need to be offset by surface treatments to protect the porous structure from fluid penetration or mechanical degradation [16].

Total and Effective Porosity

P_t (density-based) grows almost exponentially. SEM image analysis (Figure 2) confirms that P_e remains low (< 5 %) up to 30 vol %; most porosity is captive inside intact shells. At 40 – 50 vol % two extra sources appear: (i) voids between poorly wetted clusters, (ii) collapsed microspheres. The strong negative correlation ρ_exp ~ P_e (R^2 = 0.96) is plotted in Figure 2 and forms the basis for predictive mass/porosity charts used in sandwich core sizing.

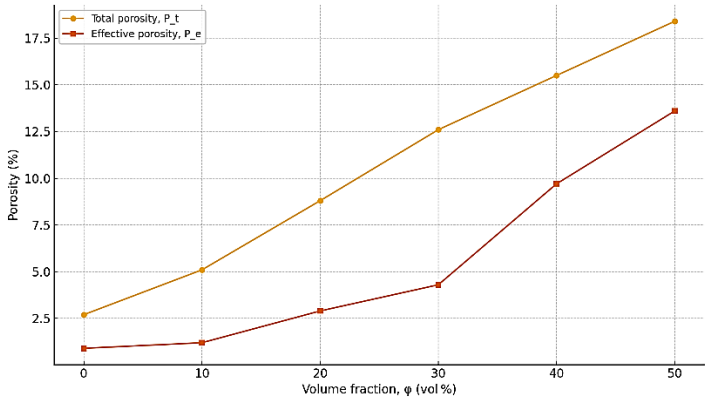

Figure 2. Porosity vs Microballoons Volume Fraction

Based on Figure 2, the graph illustrates how total porosity (P_t) and effective porosity (P_e) evolve as the filler volume fraction (φ) increases from 0 % to 50 %. P_t, which reflects all voids, both closed and open rises almost linearly, from 2.7 % to 18.4 %. This confirms that each addition of filler consistently creates new void space within the composite matrix. In contrast, P_e, the truly interconnected pores, starts much lower (0.9 %) and increases only gradually up to φ ≈ 30 % (4.3 %). Beyond this threshold, P_e jumps sharply (9.7 % at 40 % and 13.6 % at 50 %), indicating pore percolation: an open-pore network has formed, so more voids become interconnected. The difference P_t – P_e maps the fraction of closed pores; a large gap at φ ≤ 30 % signals dominance of closed cells, whereas a narrowing gap at φ ≥ 40 % marks the transition toward an open-foam structure [17]. Consequently, material at φ < 30 % is still suitable as a gas-liquid insulator because closed pores dominate, while at φ ≥ 40 %, permeability and thermal/acoustic conductivity will rise markedly as open pores facilitate fluid flow and heat transfer. Therefore, the critical point of 35–40 vol % can be recognized as the engineering boundary between “closed-cell” and “open-cell” composites, which must be considered when balancing mechanical strength, insulation, and transport properties [18].

Flexural Performance

Strength and modulus climb moderately up to 30 vol %, thanks to efficient load transfer across intact spheres. ANOVA/Tukey (α = 0.05) verifies that 30 vol % is significantly superior to 0–20 % ($p < 0.01$). The sharp fall at 40–50 vol % aligns with the surge in P_e: voids and fractured shells act as stress concentrators, initiating premature failure [19].

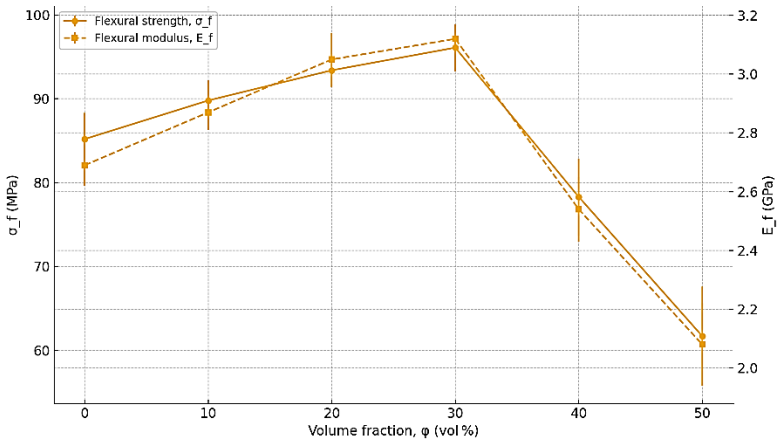

Figure 3. Flexural performance vs Microballoons Volume Fraction

Based on Figure 3, the flexural performance of the composite shows a "peak-then-drop" pattern as the filler volume fraction (φ) increases. In the range of 0–30 vol%, the addition of filler successfully increased the flexural strength (σ_f) from 85 ± 3 MPa to 96 ± 3 MPa and the flexural modulus (E_f) from 2.69 ± 0.07 GPa to 3.12 ± 0.05 GPa. This increase indicates efficient interphase stress transfer due to the uniform distribution of the filler and good matrix-filler adhesion, allowing the filler to act as a micro-supporting reinforcer. However, above 30 vol%, a saturation point is reached: particle aggregation, increased porosity, and weakened interfacial bonding trigger a drastic decline at φ = 50%, σ_f drops by 35%, and E_f decreases by 33% compared to the peak value. This behavior recommends a practical limit around 25–30 vol% for structural applications that require optimal strength and stiffness; exceeding this limit, the reinforcing

benefits are replaced by the occurrence of micro-defects that become weak points when the composite is subjected to flexural loading [20].

CONCLUSION

The composite material's performance is significantly influenced by the volume fraction of microballoons (φ), with varying effects on density, porosity, and flexural properties. The density of the composite decreases nearly linearly with increasing microballoon content, with a reduction of around 45% at φ = 50%. This suggests that the lightweight nature of microballoons effectively reduces the overall density. The relationship between total porosity (P_t) and effective porosity (P_e) also follows distinct trends. While total porosity increases almost linearly, effective porosity begins to increase sharply after φ = 30%, indicating the formation of an interconnected pore network. This transition is critical for determining the material's suitability for insulation or structural applications. Materials with φ < 30% maintain closed pores, making them suitable for gas-liquid insulation, while those with φ ≥ 40% exhibit increased permeability and reduced insulation properties. Flexural Performance: The composite's flexural strength and modulus increase up to 30 vol% due to efficient stress transfer across intact spheres, making the material more robust. However, beyond this point, a sharp decline in both strength and modulus occurs due to the aggregation of particles, increased porosity, and weakened interfacial bonding. The drop in performance at φ ≥ 40% emphasizes the importance of limiting the filler content to 25–30% for applications requiring high strength and stiffness. In conclusion, for structural applications, the composite material should ideally have a microballoon volume fraction of around 25–30% to balance low density with adequate mechanical properties. For insulation purposes, higher filler content can be used, but the increase in porosity must be carefully managed to avoid compromising material integrity.

ACKNOWLEDGMENT

Thanks to Faculty of Engineering for funding this research with Contract Number: 136.14.4/UN37/PPK.05/2025.

REFERENCES

[1] John B, Nair CR. Thermosetting polymer based syntactic foams: an overview. Handbook of thermoset plastics. 2022 Jan 1:801-32.

[2] Anirudh S, Jayalakshmi CG, Anand A, Kandasubramanian B, Ismail SO. Epoxy/hollow glass microsphere syntactic foams for structural and functional application-A review. European Polymer Journal. 2022 May 15:171:111163.

[3] Truelock D, Lavroff J, Pearson D, Czaban Z, Luo H, Wang F, Catipovic I, Begovic E, Takaoka Y, Loureiro C, Song CY. Committee v. 5: Special vessels. InInternational Ship and Offshore Structures Congress 2022 Sep 11 (p. D011S001R006). SNAME.

[4] Cao S, Ma N, Zhang Y, Bo R, Lu Y. Fabrication, mechanical properties, and multifunctionalities of particle reinforced foams: A review. Thin-Walled Structures. 2023 May 1;186:110678.

[5] Sáez-Pérez MP, Brümmer M, Durán-Suárez JA. A review of the factors affecting the properties and performance of hemp aggregate concretes. Journal of Building Engineering. 2020 Sep 1;31:101323.

[6] Mi H. Functional Polymer Foams: Green Fabrication Methods, Performance and Applications. John Wiley & Sons; 2024 Nov 13.

[7] Gurung BD, Kakar S. An overview on microspheres. Int J Health Clin Res. 2020;3(1):11-24.

[8] Karasu B, Demirel İ, Öztuvan A, Özdemir B. Glass microspheres. El-Cezeri. 2019 Sep 30;6(3):613-41.

[9] Berkland C, Kipper MJ, Narasimhan B, Kim KK, Pack DW. Microsphere size, precipitation kinetics and drug distribution control drug release from biodegradable polyanhydride microspheres. Journal of Controlled Release. 2004 Jan 8;94(1):129-41.

[10] Wu X, Gao Y, Wang Y, Fan R, Ali Z, Yu J, Yang K, Sun K, Li X, Lei Y, Shi D. Recent developments on epoxy-based syntactic foams for deep sea exploration. Journal of Materials Science. 2021 Jan;56:2037-76.

[11] Zhu Z, Huo W, Sun H, Ma B, Yang L. Correlations between unconfined compressive strength, sorptivity and pore structures for geopolymer based on SEM and MIP measurements. Journal of Building Engineering. 2023 May 15;67:106011.

[12] Kovářík T, Hájek J, Hervert T, Deshmukh K, Pola M, Jansa Z, Beneš J, Svoboda M. Silica-based geopolymer spherical beads: Influence of viscosity on porosity architecture. Cement and Concrete Composites. 2021 Nov 1;124:104261.

[13] Lu Z, Zhou WH, Yin ZY. Effect of viscosity on slurry infiltration in granular media. International Journal of Geomechanics. 2022 Sep 1;22(9):04022138.
[14] Han Z, Zhou M, Jing K, Chu C, Zhang Y, Tian B, Li ZA, He W, Song L. Effect of Mg addition on the microstructure and mechanical properties of Cu-Ti-Zr alloy. Journal of Alloys and Compounds. 2024 Nov 5;1004:175897.
[15] Vladimirova E, Gong M. Advancements and applications of wood-based sandwich panels in modern construction. Buildings. 2024 Jul 31;14(8):2359.
[16] Wang X, Tian W, Ye Y, Chen Y, Wu W, Jiang S, Wang Y, Han X. Surface modifications towards superhydrophobic wood-based composites: Construction strategies, functionalization, and perspectives. Advances in colloid and interface science. 2024 Mar 28:103142.
[17] Yu W, Kanj MY. Review of foam stability in porous media: The effect of coarsening. Journal of Petroleum Science and Engineering. 2022 Jan 1;208:109698.
[18] Iqbal S, Kamiński M. Review study on mechanical properties of cellular materials. Materials. 2024 Jun 2;17(11):2682.
[19] Stevenson ME, Umberger PD, Uchneat SF. Fracture appearance and mechanisms of deformation and fracture. InFailure analysis and prevention 2021 Jan 15 (pp. 273-303). ASM International.
[20] Ashebir DA, Hendlmeier A, Dunn M, Arablouei R, Lomov SV, Di Pietro A, Nikzad M. Detecting multi-scale defects in material extrusion additive manufacturing of fiber-reinforced thermoplastic composites: a review of challenges and advanced non-destructive testing techniques. Polymers. 2024 Oct 24;16(21):2986.